Supplement of

Compensating biases in CMIP6 TOA radiative-flux trends and their implications for EEI-based constraints on equilibrium climate sensitivity

Takuro Michibata[1] and Momoka Nakanishi[1,2]

[1]Research Institute for Applied Mechanics, Kyushu University, Fukuoka 816-8580, Japan
[2]Interdisciplinary Graduate School of Engineering Sciences, Kyushu University, Fukuoka 816-8580, Japan

Correspondence: Takuro Michibata (michibata@riam.kyushu-u.ac.jp)

This PDF file includes: Tables S1 and S2, and Figures S1 to S5

Table S1. CMIP6 models used in this study.

	Model name	Run name	ECS	Source	Reference
1	ACCESS-CM2	r1i1p1f1_gn	4.7	Australia	Bi et al. (2020)
2	ACCESS-ESM1-5	r1i1p1f1_gn	3.9	Australia	Ziehn et al. (2020)
3	AWI-CM-1-1-LR	r1i1p1f1_gn	3.3	Germany	Semmler et al. (2020)
4	BCC-ESM1	r1i1p1f1_gn	3.3	China	Wu et al. (2020)
5	BCC-CSM2-MR	r1i1p1f1_gn	3.0	China	Wu et al. (2019)
6	CAMS-CSM1-0	r1i1p1f1_gn	2.3	China	Rong et al. (2018)
7	CanESM5	r1i1p1f1_gn	5.6	Canada	Swart et al. (2019)
8	CESM2	r1i1p1f1_gn	5.2	USA	Danabasoglu et al. (2020)
9	CESM2-WACCM	r1i1p1f1_gn	4.7	USA	Danabasoglu et al. (2020)
10	CNRM-CM6-1	r1i1p1f2_gr	4.9	France	Voldoire et al. (2019)
11	CNRM-CM6-1-HR	r1i1p1f2_gr	4.3	France	Voldoire et al. (2019)
12	CNRM-ESM2-1	r1i1p1f2_gn	4.8	France	Voldoire et al. (2019)
13	E3SM-1-0	r1i1p1f1_gr	5.3	USA	Golaz et al. (2019))
14	EC-Earth3	r1i1p1f1_gr	4.1	Europe	Döscher et al. (2022)
15	EC-Earth3-Veg	r1i1p1f1_gr	4.3	Europe	Döscher et al. (2022)
16	FGOALS-f3-L	r1i1p1f1_gr	3.0	China	He et al. (2019)
17	GFDL-CM4	r1i1p1f1_gr	3.9	USA	Held et al. (2019)
18	GFDL-ESM4	r1i1p1f1_gr	2.6	USA	Dunne et al. (2020)
19	GISS-E2-1-G	r1i1p1f2_gn	2.7	USA	Kelley et al. (2020)
20	GISS-E2-1-H	r1i1p1f2_gn	3.1	USA	Kelley et al. (2020)
21	HadGEM3-GC31-LL	r1i1p1f3_gn	5.6	UK	Kuhlbrodt et al. (2018)
22	INM-CM4-8	r1i1p1f1_gr	1.8	Russia	Volodin et al. (2018)
23	INM-CM5-0	r1i1p1f1_gr	1.9	Russia	Volodin et al. (2017)
24	IPSL-CM6A-LR	r1i1p1f1_gr	4.6	France	Boucher et al. (2020)
25	MIROC-ES2L	r1i1p1f2_gn	2.7	Japan	Hajima et al. (2020)
26	MIROC6	r1i1p1f1_gn	2.6	Japan	Tatebe et al. (2019)
27	MPI-ESM1-2-HAM	r1i1p1f1_gn	3.0	Germany	Neubauer et al. (2019)
28	MPI-ESM1-2-HR	r1i1p1f1_gn	3.0	Germany	Müller et al. (2018)
29	MRI-ESM2-0	r1i1p1f1_gn	3.1	Japan	Yukimoto et al. (2019)
30	NESM3	r1i1p1f1_gn	4.8	China	Cao et al. (2018)
31	NorESM2-LM	r1i1p1f1_gn	2.6	Norway	Seland et al. (2020)
32	NorESM2-MM	r1i1p1f1_gn	2.4	Norway	Seland et al. (2020)
33	SAM0-UNICON	r1i1p1f1_gn	3.7	Korea	Park et al. (2019)
34	UKESM1-0-LL	r1i1p1f2_gn	5.4	UK	Sellar et al. (2019)

Table S2. Summary statistics of the trends in TOA radiative-flux ($\mathrm{W\,m^{-2}\,dec^{-1}}$) and total cloud coverage (TCC; $\mathrm{\%\,dec^{-1}}$) obtained from 34 CMIP6 models and CERES satellite retrievals. Radiative-flux trends are reported for all-sky, clear-sky, and CRE for the net, SW, and LW components, respectively.

	Model name	$\mathrm{Net^{all}}$	$\mathrm{SW^{all}}$	$\mathrm{LW^{all}}$	$\mathrm{Net^{clr}}$	$\mathrm{SW^{clr}}$	$\mathrm{LW^{clr}}$	$\mathrm{Net^{CRE}}$	$\mathrm{SW^{CRE}}$	$\mathrm{LW^{CRE}}$	TCC
1	ACCESS-CM2	0.21	0.57	-0.36	0.13	0.30	-0.17	0.08	0.27	-0.18	-0.32
2	ACCESS-ESM1-5	0.51	0.43	0.09	0.23	0.03	0.20	0.28	0.40	-0.12	-0.21
3	AWI-CM-1-1-LR	-0.21	-0.22	0.02	-0.17	-0.22	0.05	-0.03	0.00	-0.04	0.13
4	BCC-ESM1	0.06	0.00	0.07	0.28	0.06	0.22	-0.22	-0.06	-0.16	-0.03
5	BCC-CSM2-MR	0.31	0.09	0.22	0.42	0.22	0.19	-0.11	-0.14	0.03	0.04
6	CAMS-CSM1-0	0.06	0.05	0.01	-0.12	-0.17	0.05	0.18	0.22	-0.04	-0.17
7	CanESM5	0.27	0.59	-0.32	0.11	0.48	-0.36	0.15	0.11	0.04	0.06
8	CESM2	-0.07	-0.07	0.00	0.24	0.05	0.19	-0.32	-0.12	-0.19	-0.04
9	CESM2-WACCM	0.68	0.56	0.12	0.36	0.08	0.28	0.31	0.48	-0.16	-0.32
10	CNRM-CM6-1	0.33	0.28	0.05	0.27	0.18	0.08	0.06	0.09	-0.03	-0.05
11	CNRM-CM6-1-HR	0.32	0.36	-0.03	0.30	0.36	-0.06	0.03	-0.01	0.03	-0.07
12	CNRM-ESM2-1	0.19	0.12	0.07	0.14	0.15	-0.02	0.05	-0.03	0.09	0.09
13	E3SM-1-0	-0.23	0.30	-0.53	-0.23	0.15	-0.38	0.00	0.14	-0.14	-0.15
14	EC-Earth3	0.12	0.49	-0.37	0.20	0.50	-0.30	-0.09	-0.01	-0.07	-0.06
15	EC-Earth3-Veg	0.25	0.27	-0.02	0.19	0.06	0.13	0.07	0.21	-0.15	-0.33
16	FGOALS-f3-L	-0.04	-0.11	0.07	0.15	-0.06	0.21	-0.19	-0.05	-0.13	0.14
17	GFDL-CM4	0.08	0.15	-0.08	0.12	0.15	-0.03	-0.04	0.00	-0.05	-0.10
18	GFDL-ESM4	0.12	0.13	-0.02	0.03	-0.08	0.11	0.09	0.22	-0.12	-0.17
19	GISS-E2-1-G	0.17	-0.15	0.31	0.31	-0.01	0.31	-0.14	-0.14	0.00	0.11
20	GISS-E2-1-H	0.14	0.07	0.07	0.25	0.12	0.12	-0.10	-0.06	-0.05	0.26
21	HadGEM3-GC31-LL	0.21	0.96	-0.75	-0.07	0.35	-0.43	0.28	0.61	-0.32	-0.68
22	INM-CM4-8	-0.10	-0.10	-0.01	-0.02	-0.12	0.11	-0.09	0.03	-0.12	-0.32
23	INM-CM5-0	0.00	-0.29	0.29	0.04	-0.33	0.37	-0.04	0.04	-0.08	0.00
24	IPSL-CM6A-LR	0.17	0.52	-0.35	0.10	0.35	-0.25	0.07	0.17	-0.10	-0.3
25	MIROC-ES2L	0.32	0.29	0.03	0.25	0.11	0.14	0.07	0.18	-0.11	-0.24
26	MIROC6	-0.23	0.04	-0.27	-0.01	0.07	-0.08	-0.22	-0.03	-0.19	0.09
27	MPI-ESM1-2-HAM	0.15	0.10	0.05	0.14	-0.05	0.19	0.01	0.15	-0.15	-0.11
28	MPI-ESM1-2-HR	0.16	0.31	-0.14	0.19	0.34	-0.15	-0.03	-0.03	0.00	-0.11
29	MRI-ESM2-0	0.24	0.25	0.00	0.34	0.30	0.04	-0.09	-0.05	-0.04	-0.01
30	NESM3	0.04	0.26	-0.22	0.06	0.34	-0.29	-0.02	-0.09	0.07	-0.09
31	NorESM2-LM	0.71	1.20	-0.49	-0.08	0.16	-0.24	0.80	1.04	-0.25	-0.64
32	NorESM2-MM	-0.01	0.16	-0.17	0.00	-0.07	0.07	-0.01	0.23	-0.25	-0.20
33	SAM0-UNICON	0.42	0.59	-0.17	0.28	0.25	0.03	0.14	0.34	-0.20	-0.39
34	UKESM1-0-LL	0.33	0.79	-0.47	0.02	0.26	-0.25	0.31	0.53	-0.22	-0.30
	Multi-Model Mean	0.17	0.26	-0.10	0.13	0.13	0.00	0.04	0.14	-0.10	-0.13
	CERES (2001-2024)	0.45	0.83	-0.39	0.38	0.38	0.00	0.06	0.45	-0.39	-0.11
	CERES (2001-2014)	0.37	0.27	0.09	0.52	0.19	0.32	-0.15	0.08	-0.23	-0.19

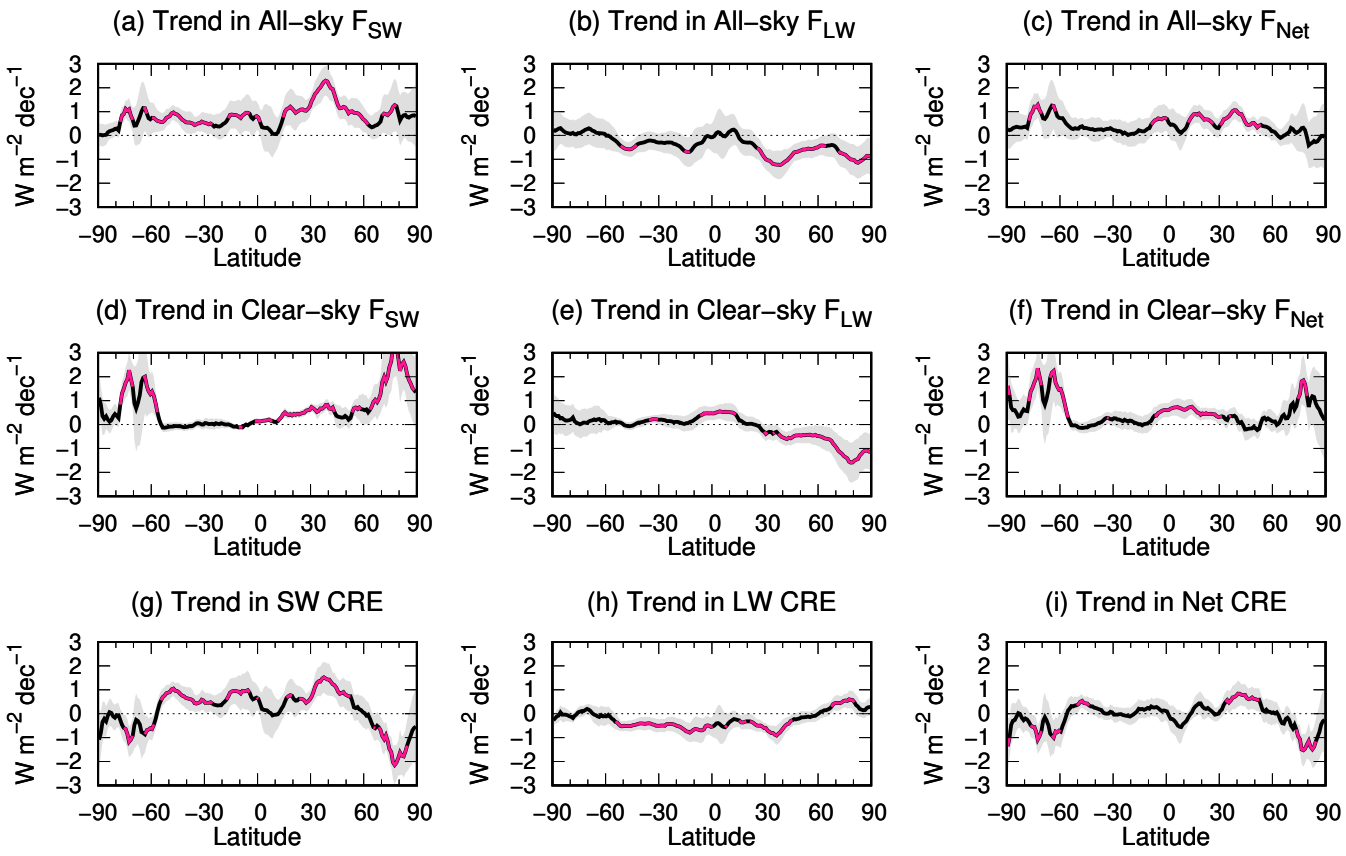


Figure S1. Zonal distributions of radiative-flux trends. Trends for (**a**) all-sky SW, (**b**) all-sky LW, (**c**) all-sky net, (**d**) clear-sky SW, (**e**) clear-sky LW, (**f**) clear-sky net, (**g**) SW CRE, (**h**) LW CRE, and (**i**) net CRE trends retrieved from the CERES satellite for the period January 2001–December 2024. Grey shading provides the 95% confidence interval of the trend, and red regions indicate statistically significant trends at the 95% confidence level.

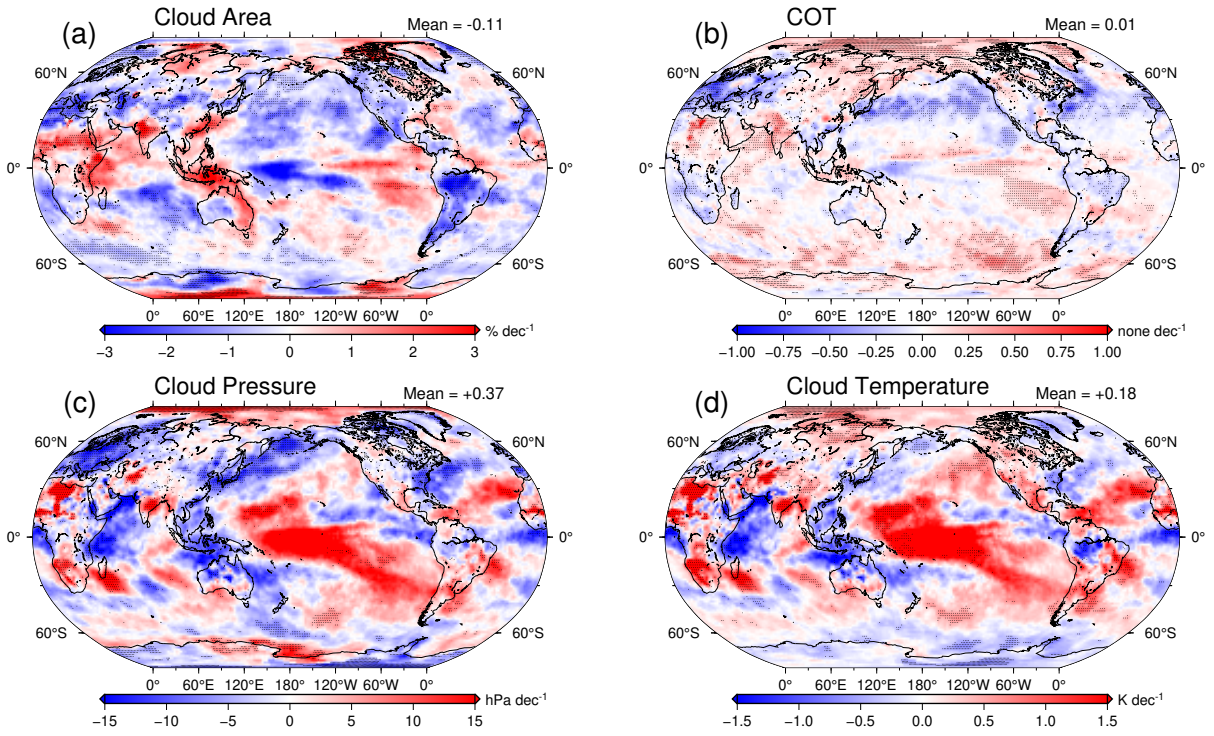


Figure S2. Geographical distributions of cloud-property trends derived from CERES–MODIS retrievals. Trends for (**a**) cloud areal fraction, (**b**) cloud optical thickness, (**c**) cloud effective pressure, and (**d**) cloud effective temperature for the period January 2001–December 2024. Global mean values are provided at the top right of each panel. Dots indicate regions where trends differ significantly from zero at the 95% confidence level. Units are shown in each panel.

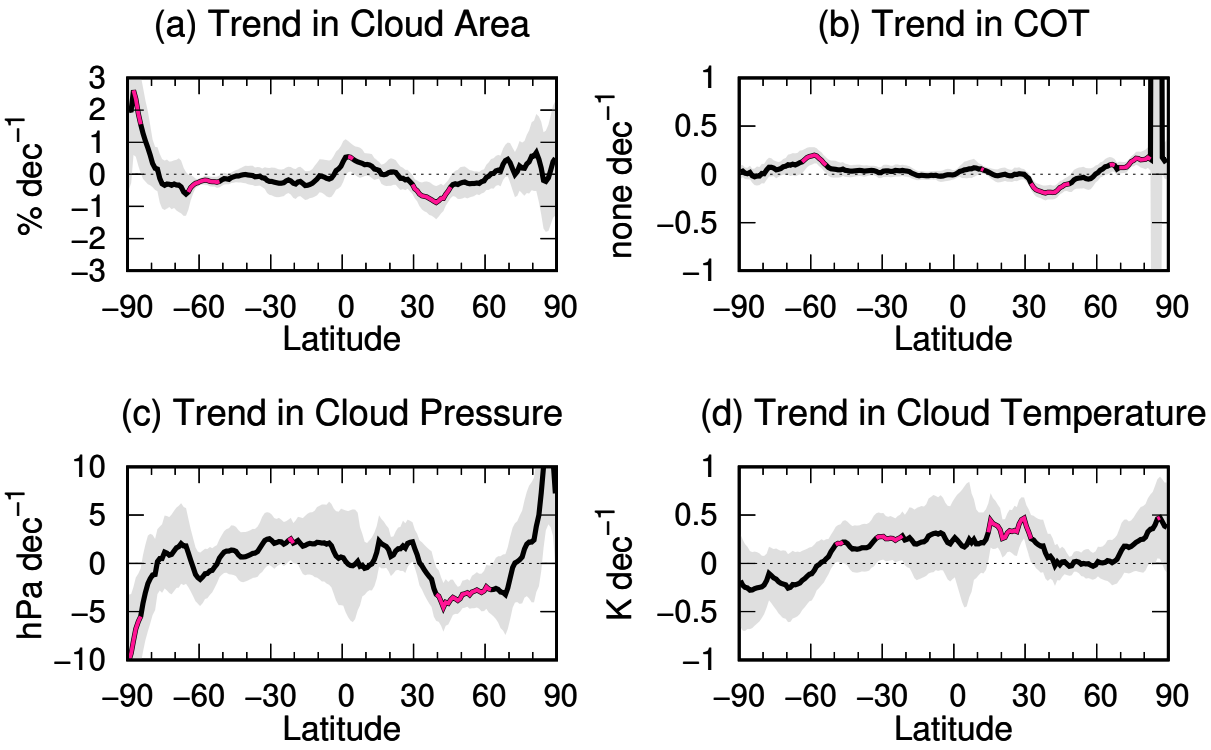


Figure S3. Zonal distributions of cloud trends. Trends for (**a**) cloud areal fraction, (**b**) cloud optical thickness, (**c**) cloud effective pressure, and (**d**) cloud effective temperature for the period January 2001–December 2024. Grey shading provides the 95% confidence interval of the trend, and red regions indicate statistically significant trends at the 95% confidence level.

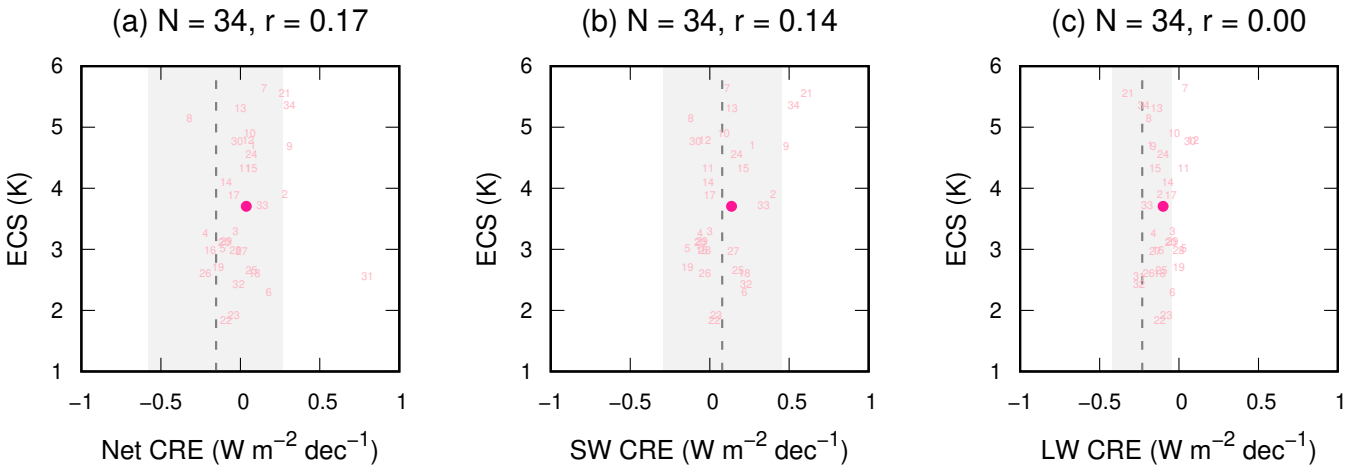


Figure S4. Relationship between ECS and CRE trends. Trends for (**a**) net CRE, (**b**) SW CRE, and (**c**) LW CER trends for CMIP6 models. Numbers correspond to models summarized in Table S2, and the circle indicates the multimodel mean. Dashed lines with grey shading show the CERES satellite estimate with a 95% confidence interval. The correlation coefficient between the CRE trend and ECS (r) is shown in each panel.

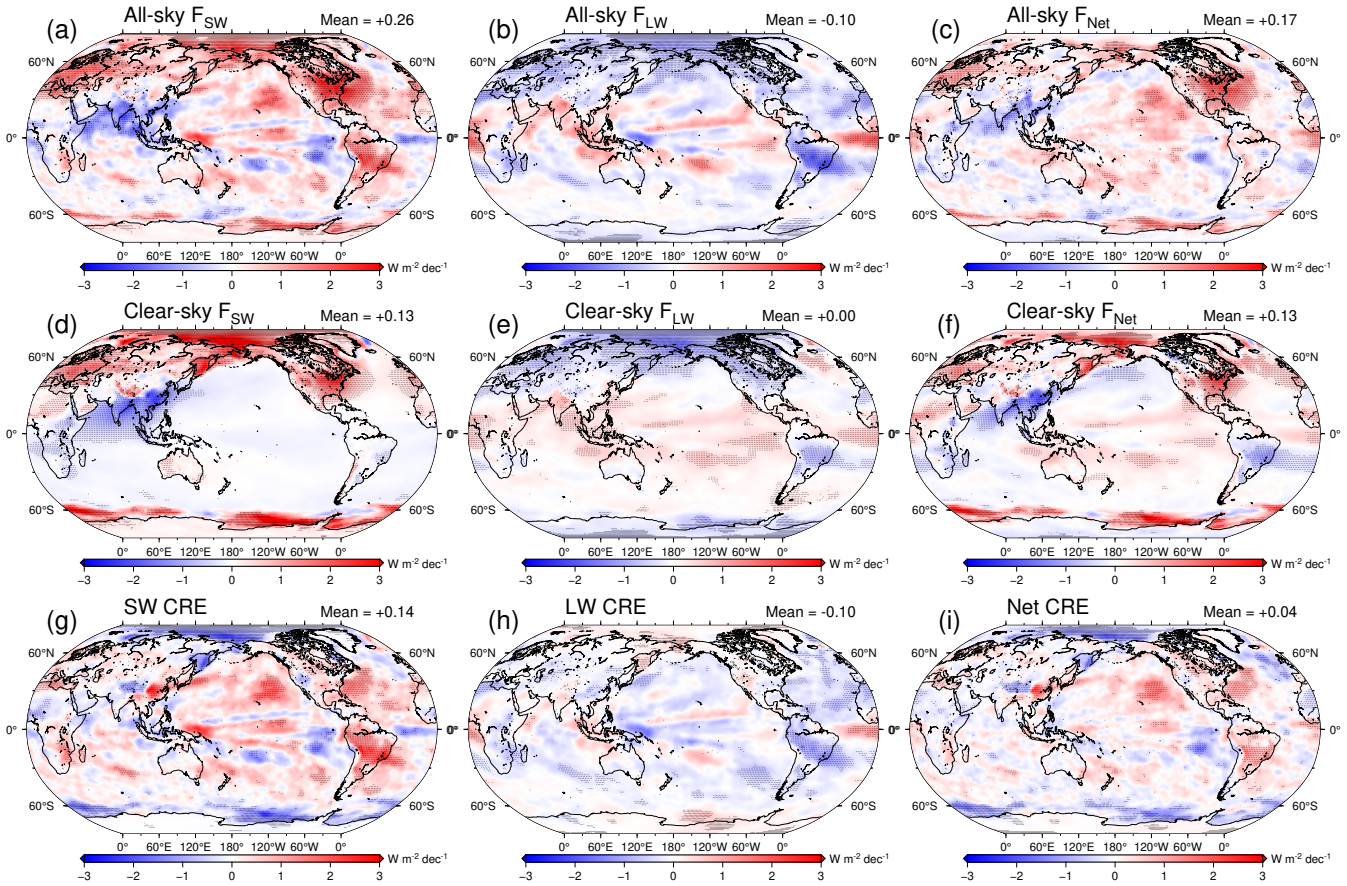


Figure S5. Geographical distributions of multimodel-mean TOA radiative-flux trends simulated by 34 CMIP6 models. Trends for (**a**) all-sky SW, (**b**) all-sky LW, (**c**) all-sky net, (**d**) clear-sky SW, (**e**) clear-sky LW, (**f**) clear-sky net, (**g**) SW CRE, (**h**) LW CRE, and (**i**) net CRE for the period January 2001–December 2014. Global mean values are provided at the top right of each panel. Dots indicate regions where trends differ significantly from zero at the 95% confidence level. Units are $\mathrm{W\,m^{-2}\,dec^{-1}}$, positive downward.

References from the Supporting Information

Bi, D., Dix, M., Marsland, S., O'farrell, S., Sullivan, A., Bodman, R., Law, R., Harman, I., Srbinovsky, J., Rashid, H. A., Dobrohotoff, P., Mackallah, C., Yan, H., Hirst, A., Savita, A., Dias, F. B., Woodhouse, M., Fiedler, R., and Heerdegen, A.: Configuration and spin-up of ACCESS-CM2, the new generation Australian Community Climate and Earth System Simulator Coupled Model, Journal of Southern Hemisphere Earth Systems Science, 70, 225–251, https://doi.org/10.1071/ES19040, 2020.

Boucher, O., Servonnat, J., Albright, A. L., Aumont, O., Balkanski, Y., Bastrikov, V., Bekki, S., Bonnet, R., Bony, S., Bopp, L., Braconnot, P., Brockmann, P., Cadule, P., Caubel, A., Cheruy, F., Codron, F., Cozic, A., Cugnet, D., D'Andrea, F., Davini, P., de Lavergne, C., Denvil, S., Deshayes, J., Devilliers, M., Ducharne, A., Dufresne, J. L., Dupont, E., Éthé, C., Fairhead, L., Falletti, L., Flavoni, S., Foujols, M. A., Gardoll, S., Gastineau, G., Ghattas, J., Grandpeix, J. Y., Guenet, B., Guez, Lionel, E., Guilyardi, E., Guimberteau, M., Hauglustaine, D., Hourdin, F., Idelkadi, A., Joussaume, S., Kageyama, M., Khodri, M., Krinner, G., Lebas, N., Levavasseur, G., Lévy, C., Li, L., Lott, F., Lurton, T., Luyssaert, S., Madec, G., Madeleine, J. B., Maignan, F., Marchand, M., Marti, O., Mellul, L., Meurdesoif, Y., Mignot, J., Musat, I., Ottlé, C., Peylin, P., Planton, Y., Polcher, J., Rio, C., Rochetin, N., Rousset, C., Sepulchre, P., Sima, A., Swingedouw, D., Thiéblemont, R., Traore, A. K., Vancoppenolle, M., Vial, J., Vialard, J., Viovy, N., and Vuichard, N.: Presentation and Evaluation of the IPSL-CM6A-LR Climate Model, Journal of Advances in Modeling Earth Systems, 12, e2019MS002 010, https://doi.org/10.1029/2019MS002010, 2020.

Cao, J., Wang, B., Yang, Y. M., Ma, L., Li, J., Sun, B., Bao, Y., He, J., Zhou, X., and Wu, L.: The NUIST Earth System Model (NESM) version 3: Description and preliminary evaluation, Geoscientific Model Development, 11, 2975–2993, https://doi.org/10.5194/gmd-11-2975-2018, 2018.

Danabasoglu, G., Lamarque, J. F., Bacmeister, J., Bailey, D. A., DuVivier, A. K., Edwards, J., Emmons, L. K., Fasullo, J., Garcia, R., Gettelman, A., Hannay, C., Holland, M. M., Large, W. G., Lauritzen, P. H., Lawrence, D. M., Lenaerts, J. T., Lindsay, K., Lipscomb, W. H., Mills, M. J., Neale, R., Oleson, K. W., Otto-Bliesner, B., Phillips, A. S., Sacks, W., Tilmes, S., van Kampenhout, L., Vertenstein, M., Bertini, A., Dennis, J., Deser, C., Fischer, C., Fox-Kemper, B., Kay, J. E., Kinnison, D., Kushner, P. J., Larson, V. E., Long, M. C., Mickelson, S., Moore, J. K., Nienhouse, E., Polvani, L., Rasch, P. J., and Strand, W. G.: The Community Earth System Model Version 2 (CESM2), Journal of Advances in Modeling Earth Systems, 12, e2019MS001 916, https://doi.org/10.1029/2019MS001916, 2020.

Döscher, R., Acosta, M., Alessandri, A., Anthoni, P., Arsouze, T., Bergman, T., Bernardello, R., Boussetta, S., Caron, L. P., Carver, G., Castrillo, M., Catalano, F., Cvijanovic, I., Davini, P., Dekker, E., Doblas-Reyes, F. J., Docquier, D., Echevarria, P., Fladrich, U., Fuentes-Franco, R., Gröger, M., Hardenberg, J. V., Hieronymus, J., Karami, M. P., Keskinen, J. P., Koenigk, T., Makkonen, R., Massonnet, F., Ménégoz, M., Miller, P. A., Moreno-Chamarro, E., Nieradzik, L., Van Noije, T., Nolan, P., O'donnell, D., Ollinaho, P., Van Den Oord, G., Ortega, P., Prims, O. T., Ramos, A., Reerink, T., Rousset, C., Ruprich-Robert, Y., Le Sager, P., Schmith, T., Schrödner, R., Serva, F., Sicardi, V., Sloth Madsen, M., Smith, B., Tian, T., Tourigny, E., Uotila, P., Vancoppenolle, M., Wang, S., Wårlind, D., Willén, U., Wyser, K., Yang, S., Yepes-Arbós, X., and Zhang, Q.: The EC-Earth3 Earth system model for the Coupled Model Intercomparison Project 6, Geoscientific Model Development, 15, 2973–3020, https://doi.org/10.5194/gmd-15-2973-2022, 2022.

Dunne, J. P., Horowitz, L. W., Adcroft, A. J., Ginoux, P., Held, I. M., John, J. G., Krasting, J. P., Malyshev, S., Naik, V., Paulot, F., Shevliakova, E., Stock, C. A., Zadeh, N., Balaji, V., Blanton, C., Dunne, K. A., Dupuis, C., Durachta, J., Dussin, R., Gauthier, P. P., Griffies, S. M., Guo, H., Hallberg, R. W., Harrison, M., He, J., Hurlin, W., McHugh, C., Menzel, R., Milly, P. C., Nikonov, S., Paynter, D. J., Ploshay, J., Radhakrishnan, A., Rand, K., Reichl, B. G., Robinson, T., Schwarzkopf, D. M., Sentman, L. T., Underwood, S., Vahlenkamp, H., Winton, M., Wittenberg, A. T., Wyman, B., Zeng, Y., and Zhao, M.: The GFDL Earth System Model Version 4.1 (GFDL-ESM 4.1): Overall

Coupled Model Description and Simulation Characteristics, Journal of Advances in Modeling Earth Systems, 12, e2019MS002 015, https://doi.org/10.1029/2019MS002015, 2020.

Golaz, J. C., Caldwell, P. M., Van Roekel, L. P., Petersen, M. R., Tang, Q., Wolfe, J. D., Abeshu, G., Anantharaj, V., Asay-Davis, X. S., Bader, D. C., Baldwin, S. A., Bisht, G., Bogenschutz, P. A., Branstetter, M., Brunke, M. A., Brus, S. R., Burrows, S. M., Cameron-Smith, P. J., Donahue, A. S., Deakin, M., Easter, R. C., Evans, K. J., Feng, Y., Flanner, M., Foucar, J. G., Fyke, J. G., Griffin, B. M., Hannay, C., Harrop, B. E., Hoffman, M. J., Hunke, E. C., Jacob, R. L., Jacobsen, D. W., Jeffery, N., Jones, P. W., Keen, N. D., Klein, S. A., Larson, V. E., Leung, L. R., Li, H. Y., Lin, W., Lipscomb, W. H., Ma, P. L., Mahajan, S., Maltrud, M. E., Mametjanov, A., McClean, J. L., McCoy, R. B., Neale, R. B., Price, S. F., Qian, Y., Rasch, P. J., Reeves Eyre, J. E., Riley, W. J., Ringler, T. D., Roberts, A. F., Roesler, E. L., Salinger, A. G., Shaheen, Z., Shi, X., Singh, B., Tang, J., Taylor, M. A., Thornton, P. E., Turner, A. K., Veneziani, M., Wan, H., Wang, H., Wang, S., Williams, D. N., Wolfram, P. J., Worley, P. H., Xie, S., Yang, Y., Yoon, J. H., Zelinka, M. D., Zender, C. S., Zeng, X., Zhang, C., Zhang, K., Zhang, Y., Zheng, X., Zhou, T., and Zhu, Q.: The DOE E3SM Coupled Model Version 1: Overview and Evaluation at Standard Resolution, Journal of Advances in Modeling Earth Systems, 11, 2089–2129, https://doi.org/10.1029/2018MS001603, 2019.

Hajima, T., Watanabe, M., Yamamoto, A., Tatebe, H., Noguchi, M. A., Abe, M., Ohgaito, R., Ito, A., Yamazaki, D., Okajima, H., Ito, A., Takata, K., Ogochi, K., Watanabe, S., and Kawamiya, M.: Development of the MIROC-ES2L Earth system model and the evaluation of biogeochemical processes and feedbacks, Geoscientific Model Development, 13, 2197–2244, https://doi.org/10.5194/gmd-13-2197-2020, 2020.

He, B., Bao, Q., Wang, X., Zhou, L., Wu, X., Liu, Y., Wu, G., Chen, K., He, S., Hu, W., Li, J., Li, J., Nian, G., Wang, L., Yang, J., Zhang, M., and Zhang, X.: CAS FGOALS-f3-L Model Datasets for CMIP6 Historical Atmospheric Model Intercomparison Project Simulation, Advances in Atmospheric Sciences, 36, 771–778, https://doi.org/10.1007/s00376-019-9027-8, 2019.

Held, I. M., Guo, H., Adcroft, A., Dunne, J. P., Horowitz, L. W., Krasting, J., Shevliakova, E., Winton, M., Zhao, M., Bushuk, M., Wittenberg, A. T., Wyman, B., Xiang, B., Zhang, R., Anderson, W., Balaji, V., Donner, L., Dunne, K., Durachta, J., Gauthier, P. P., Ginoux, P., Golaz, J. C., Griffies, S. M., Hallberg, R., Harris, L., Harrison, M., Hurlin, W., John, J., Lin, P., Lin, S. J., Malyshev, S., Menzel, R., Milly, P. C., Ming, Y., Naik, V., Paynter, D., Paulot, F., Rammaswamy, V., Reichl, B., Robinson, T., Rosati, A., Seman, C., Silvers, L. G., Underwood, S., and Zadeh, N.: Structure and Performance of GFDL's CM4.0 Climate Model, Journal of Advances in Modeling Earth Systems, 11, 3691–3727, https://doi.org/10.1029/2019MS001829, 2019.

Kelley, M., Schmidt, G. A., Nazarenko, L. S., Bauer, S. E., Ruedy, R., Russell, G. L., Ackerman, A. S., Aleinov, I., Bauer, M., Bleck, R., Canuto, V., Cesana, G., Cheng, Y., Clune, T. L., Cook, B. I., Cruz, C. A., Del Genio, A. D., Elsaesser, G. S., Faluvegi, G., Kiang, N. Y., Kim, D., Lacis, A. A., Leboissetier, A., LeGrande, A. N., Lo, K. K., Marshall, J., Matthews, E. E., McDermid, S., Mezuman, K., Miller, R. L., Murray, L. T., Oinas, V., Orbe, C., García-Pando, C. P., Perlwitz, J. P., Puma, M. J., Rind, D., Romanou, A., Shindell, D. T., Sun, S., Tausnev, N., Tsigaridis, K., Tselioudis, G., Weng, E., Wu, J., and Yao, M. S.: GISS-E2.1: Configurations and Climatology, Journal of Advances in Modeling Earth Systems, 12, e2019MS002 025, https://doi.org/10.1029/2019MS002025, 2020.

Kuhlbrodt, T., Jones, C. G., Sellar, A., Storkey, D., Blockley, E., Stringer, M., Hill, R., Graham, T., Ridley, J., Blaker, A., Calvert, D., Copsey, D., Ellis, R., Hewitt, H., Hyder, P., Ineson, S., Mulcahy, J., Siahaan, A., and Walton, J.: The Low-Resolution Version of HadGEM3 GC3.1: Development and Evaluation for Global Climate, Journal of Advances in Modeling Earth Systems, 10, 2865–2888, https://doi.org/10.1029/2018MS001370, 2018.

Müller, W. A., Jungclaus, J. H., Mauritsen, T., Baehr, J., Bittner, M., Budich, R., Bunzel, F., Esch, M., Ghosh, R., Haak, H., Ilyina, T., Kleine, T., Kornblueh, L., Li, H., Modali, K., Notz, D., Pohlmann, H., Roeckner, E., Stemmler, I., Tian, F., and Marotzke, J.: A Higher-

resolution Version of the Max Planck Institute Earth System Model (MPI-ESM1.2-HR), Journal of Advances in Modeling Earth Systems, 10, 1383–1413, https://doi.org/10.1029/2017MS001217, 2018.

Neubauer, D., Ferrachat, S., Siegenthaler-Le Drian, C., Stier, P., Partridge, D. G., Tegen, I., Bey, I., Stanelle, T., Kokkola, H., and Lohmann, U.: The global aerosol-climate model ECHAM6.3-HAM2.3 – Part 2: Cloud evaluation, aerosol radiative forcing, and climate sensitivity, Geoscientific Model Development, 12, 3609–3639, https://doi.org/10.5194/gmd-2018-307, 2019.

Park, S., Shin, J., Kim, S., Oh, E., and Kim, Y.: Global climate simulated by the Seoul National University Atmosphere Model version 0 with a unified convection scheme (SAM0-UNICON), Journal of Climate, 32, 2917–2949, https://doi.org/10.1175/JCLI-D-18-0796.1, 2019.

Rong, X., Li, J., Chen, H., Xin, Y., Su, J., Hua, L., Zhou, T., Qi, Y., Zhang, Z., Zhang, G., and Li, J.: The CAMS Climate System Model and a Basic Evaluation of Its Climatology and Climate Variability Simulation, Journal of Meteorological Research, 32, 839–861, https://doi.org/10.1007/s13351-018-8058-x, 2018.

Seland, Ø., Bentsen, M., Olivié, D., Toniazzo, T., Gjermundsen, A., Graff, L. S., Debernard, J. B., Gupta, A. K., He, Y. C., Kirkeväg, A., Schwinger, J., Tjiputra, J., Schanke Aas, K., Bethke, I., Fan, Y., Griesfeller, J., Grini, A., Guo, C., Ilicak, M., Karset, I. H. H., Landgren, O., Liakka, J., Moseid, K. O., Nummelin, A., Spensberger, C., Tang, H., Zhang, Z., Heinze, C., Iversen, T., and Schulz, M.: Overview of the Norwegian Earth System Model (NorESM2) and key climate response of CMIP6 DECK, historical, and scenario simulations, Geoscientific Model Development, 13, 6165–6200, https://doi.org/10.5194/gmd-13-6165-2020, 2020.

Sellar, A. A., Jones, C. G., Mulcahy, J. P., Tang, Y., Yool, A., Wiltshire, A., O'Connor, F. M., Stringer, M., Hill, R., Palmieri, J., Woodward, S., de Mora, L., Kuhlbrodt, T., Rumbold, S. T., Kelley, D. I., Ellis, R., Johnson, C. E., Walton, J., Abraham, N. L., Andrews, M. B., Andrews, T., Archibald, A. T., Berthou, S., Burke, E., Blockley, E., Carslaw, K., Dalvi, M., Edwards, J., Folberth, G. A., Gedney, N., Griffiths, P. T., Harper, A. B., Hendry, M. A., Hewitt, A. J., Johnson, B., Jones, A., Jones, C. D., Keeble, J., Liddicoat, S., Morgenstern, O., Parker, R. J., Predoi, V., Robertson, E., Siahaan, A., Smith, R. S., Swaminathan, R., Woodhouse, M. T., Zeng, G., and Zerroukat, M.: UKESM1: Description and Evaluation of the U.K. Earth System Model, Journal of Advances in Modeling Earth Systems, 11, 4513–4558, https://doi.org/10.1029/2019MS001739, 2019.

Semmler, T., Danilov, S., Gierz, P., Goessling, H. F., Hegewald, J., Hinrichs, C., Koldunov, N., Khosravi, N., Mu, L., Rackow, T., Sein, D. V., Sidorenko, D., Wang, Q., and Jung, T.: Simulations for CMIP6 With the AWI Climate Model AWI-CM-1-1, Journal of Advances in Modeling Earth Systems, 12, e2019MS002 009, https://doi.org/10.1029/2019MS002009, 2020.

Swart, N. C., Cole, J. N., Kharin, V. V., Lazare, M., Scinocca, J. F., Gillett, N. P., Anstey, J., Arora, V., Christian, J. R., Hanna, S., Jiao, Y., Lee, W. G., Majaess, F., Saenko, O. A., Seiler, C., Seinen, C., Shao, A., Sigmond, M., Solheim, L., Von Salzen, K., Yang, D., and Winter, B.: The Canadian Earth System Model version 5 (CanESM5.0.3), Geoscientific Model Development, 12, 4823–4873, https://doi.org/10.5194/gmd-12-4823-2019, 2019.

Tatebe, H., Ogura, T., Nitta, T., Komuro, Y., Ogochi, K., Takemura, T., Sudo, K., Sekiguchi, M., Abe, M., Saito, F., Chikira, M., Watanabe, S., Mori, M., Hirota, N., Kawatani, Y., Mochizuki, T., Yoshimura, K., Takata, K., O'ishi, R., Yamazaki, D., Suzuki, T., Kurogi, M., Kataoka, T., Watanabe, M., and Kimoto, M.: Description and basic evaluation of simulated mean state, internal variability, and climate sensitivity in MIROC6, Geoscientific Model Development, 12, 2727–2765, https://doi.org/10.5194/gmd-12-2727-2019, 2019.

Voldoire, A., Saint-Martin, D., Sénési, S., Decharme, B., Alias, A., Chevallier, M., Colin, J., Guérémy, J. F., Michou, M., Moine, M. P., Nabat, P., Roehrig, R., Salas y Mélia, D., Séférian, R., Valcke, S., Beau, I., Belamari, S., Berthet, S., Cassou, C., Cattiaux, J., Deshayes, J., Douville, H., Ethé, C., Franchistéguy, L., Geoffroy, O., Lévy, C., Madec, G., Meurdesoif, Y., Msadek, R., Ribes, A., Sanchez-Gomez, E., Terray, L., and Waldman, R.: Evaluation of CMIP6 DECK Experiments With CNRM-CM6-1, Journal of Advances in Modeling Earth Systems, 11, 2177–2213, https://doi.org/10.1029/2019MS001683, 2019.

Volodin, E. M., Mortikov, E. V., Kostrykin, S. V., Galin, V. Y., Lykossov, V. N., Gritsun, A. S., Diansky, N. A., Gusev, A. V., and Iakovlev, N. G.: Simulation of the present-day climate with the climate model INMCM5, Climate Dynamics, 49, 3715–3734, https://doi.org/10.1007/s00382-017-3539-7, 2017.

Volodin, E. M., Mortikov, E. V., Kostrykin, S. V., Galin, V. Y., Lykossov, V. N., Gritsun, A. S., Diansky, N. A., Gusev, A. V., Iakovlev, N. G., Shestakova, A. A., and Emelina, S. V.: No Title, Russian Journal of Numerical Analysis and Mathematical Modelling, 33, 367–374, https://doi.org/doi:10.1515/rnam-2018-0032, 2018.

Wu, T., Lu, Y., Fang, Y., Xin, X., Li, L., Li, W., Jie, W., Zhang, J., Liu, Y., Zhang, L., Zhang, F., Zhang, Y., Wu, F., Li, J., Chu, M., Wang, Z., Shi, X., Liu, X., Wei, M., Huang, A., Zhang, Y., and Liu, X.: The Beijing Climate Center Climate System Model (BCC-CSM): The main progress from CMIP5 to CMIP6, Geoscientific Model Development, 12, 1573–1600, https://doi.org/10.5194/gmd-12-1573-2019, 2019.

Wu, T., Zhang, F., Zhang, J., Jie, W., Zhang, Y., Wu, F., Li, L., Yan, J., Liu, X., Lu, X., Tan, H., Zhang, L., Wang, J., and Hu, A.: Beijing Climate Center Earth System Model version 1 (BCC-ESM1): Model description and evaluation of aerosol simulations, Geoscientific Model Development, 13, 977–1005, https://doi.org/10.5194/gmd-13-977-2020, 2020.

Yukimoto, S., Kawai, H., Koshiro, T., Oshima, N., Yoshida, K., Urakawa, S., Tsujino, H., Deushi, M., Tanaka, T., Hosaka, M., Yabu, S., Yoshimura, H., Shindo, E., Mizuta, R., Obata, A., Adachi, Y., and Ishii, M.: The meteorological research institute Earth system model version 2.0, MRI-ESM2.0: Description and basic evaluation of the physical component, Journal of the Meteorological Society of Japan, 97, 931–965, https://doi.org/10.2151/jmsj.2019-051, 2019.

Ziehn, T., Chamberlain, M. A., Law, R. M., Lenton, A., Bodman, R. W., Dix, M., Stevens, L., Wang, Y. P., and Srbinovsky, J.: The Australian Earth System Model: ACCESS-ESM1.5, Journal of Southern Hemisphere Earth Systems Science, 70, 193–214, https://doi.org/10.1071/ES19035, 2020.